J. Phys.: Condens. Matter 6 (1994) 9853–9865. Printed in the UK

On entropy and ordering in binary hard-sphere mixtures

F Saija†, P V Giaquinta‡, G Giunta‡ and S Prestipino Giarritta§

† Dottorato di Ricerca in Fisica, Università degli Studi di Messina, CP 50, 98166 S Agata-Messina, Italy

‡ Dipartimento di Fisica, Università degli Studi di Messina, CP 50, 98166 S Agata-Messina, Italy

§ International School for Advanced Studies (SISSA/ISAS) Via Beirut n 2-4, 34013 Trieste, Italy

Received 17 May 1994, in final form 28 July 1994

Abstract. The configurational entropy of a binary mixture of unequal hard spheres is analysed over a wide range of densities and concentrations as a sum of two contributions: a pair term, s_2, arising from two-body spatial correlations, and a residual term, Δs, that is due to correlations involving more than two particles. The validity of a one-phase ordering criterion, based on the non-monotonic behaviour of Δs as a function of the total packing fraction, is investigated in relation to the phase transformations undergone by the model.

1. Introduction

A bidisperse mixture of hard spheres may exist in a surprisingly rich variety of both ordered and disordered phases whose formation is solely driven by entropic effects [1]. The phase diagram of a binary hard-sphere mixture has been investigated using computer simulation techniques [1–3] as well as by other theoretical methods, which are typically based on integral-equation [4–6] or density-functional approaches [7–12]. As is well known, the model has great relevance in the chemical physics of sterically stabilized suspensions of mesoscopic colloidal particles in a solvent [13]. The theoretical predictions of the nature of the stable solid phases formed at high density and on the existence of a spinodal instability leading to phase separation have been largely confirmed by experiments performed on colloidal suspensions [14–16].

In this paper we shall try to elucidate some aspects of the statistical thermodynamics of a hard-sphere mixture that are closely related to the interplay between entropy and ordering effects in the *fluid* phase. At a given global density and for an assigned relative concentration of the two species, the equilibrium state of the model is the state of maximum entropy. The present analysis is based on the explicit evaluation of the contribution arising from two-body spatial correlations to the entropy of the system, and is similar to an analysis that was recently carried out for monodisperse model fluids [17–19]. In general, the total excess entropy of a multicomponent system can be expressed as an infinite series:

$$s_{ex} = \sum_{n=2}^{\infty} s_n \tag{1}$$

where s_{ex} is the excess entropy per particle in units of the Boltzmann constant and the partial entropies s_n are obtained from the integrated contributions of the spatial correlations

0953-8984/94/469853+13$19.50

between n-tuples of particles. In particular, the two-body term can be written as [20]:

$$s_2 = -\tfrac{1}{2}\rho \sum_{ij} x_i x_j \int \{g_{ij}(r)\ln[g_{ij}(r)] - g_{ij}(r) + 1\}\, \mathrm{d}r \tag{2}$$

where ρ is the total number density, x_i is the mole fraction of component i ($i = 1, 2$), and the quantities $g_{ij}(r)$ are the partial pair distribution functions (PDF).

The residual multiparticle entropy

$$\Delta s \equiv s_{ex} - s_2 \tag{3}$$

despite its minor quantitative relevance in the overall balance, turns out to be a rather sensitive indicator of the structural and dynamical changes that take place in the system. In this respect, it is rather illuminating to register a change of sign (from negative to positive values) that Δs undergoes in close proximity to the freezing point of hard spheres [17]. Retrospectively, one realizes that this condition monitors a crossover in the behaviour of multiparticle correlations (specifically, those involving at least three particles) from a weakly to a strongly interacting regime. In fact, the increasing efficiency demanded in order to pack the spheres into a smaller and smaller volume ultimately sets off an *ordering* process, which initially spreads over a microscopic range of distances. It is clear that in an infinite system this cooperative phenomenon cannot be properly resolved except at a sufficiently high level of the correlation-function hierarchy [21]. As to the entropy of the system, the subtle but rather natural counterpart of such a structural rearrangement is a relative increase of configurational states that become accessible on a local scale [22]. Hence, the systematic entropy loss produced by localization ($s_2 < 0$) is tempered at high densities by the gain that is associated with the sprouting of spatial order in the fluid ($\Delta s > 0$).

There is, *a priori*, no compelling reason why the 'threshold' identified by the zero of the residual multiparticle entropy should coincide with a thermodynamic phase boundary of the system. In fact, the latter is always settled through a comparison of the free energies of two coexisting phases. The rationale behind the criterion is rather that of an intrinsic signature of the germination, in the fluid phase, of a new type of local order, an event that should be plausibly related to the macroscopic transformations that are eventually undergone by the system.

In addition to bare hard spheres, the 'one-phase' entropic criterion $\Delta s(\rho, T) = 0$ has been successfully checked along the freezing line of a Lennard-Jones liquid over a wide range of temperatures T [18, 19].

In this paper we plan to analyse the residual multiparticle entropy Δs of a binary hard-sphere mixture as a function of the equilibrium parameters (total number density and relative concentration of the two species) and of the sphere-size ratio $\alpha \equiv \sigma_2/\sigma_1$, where σ_i is the hard-core diameter of the ith component, and $\sigma_2 < \sigma_1$.

The layout of the paper is as follows. In section 2 we introduce the theoretical framework of the calculation. The results are then presented and discussed in section 3. Section 4 is devoted to concluding remarks.

2. Theory and implementation

In order to carry out an extensive analysis of Δs over the thermodynamic plane spanned by the packing fractions $\eta_i = \frac{1}{6}\pi\rho x_i\sigma_i^3$ of the two species, we resorted to the Percus–Yevick (PY) approximation [23]. As is well known, the PY recipe is a flexible first-strike tool for the calculation of the structural properties since the solution is available

in closed analytical form for a multicomponent mixture also [24]. In general, the overall agreement of the PY results with the simulation data in the case of a bidisperse hard-sphere mixture is fairly good [4,5,25,26]. The drawbacks of the approximation are similar to those found in a monodisperse system. More specifically, the values at contact of the radial distribution functions turn out to be underestimated, while their spatial oscillations are slightly shifted to larger distances. Furthermore, the first minimum in the like–like distribution functions is systematically deeper than that predicted by computer simulation and may, eventually, become negative. In particular, for values of the sphere-size ratio in the range $0.2 \lesssim \alpha \lesssim 0.74$, a window in concentration opens up where the first dip in the PDF of the larger-sized spheres becomes negative in the density range that is relevant for estimating the freezing point of the mixture. This feature clearly restricts the domain where the PY approximation may furnish physically meaningful predictions.

Some calculations of the pair entropy s_2 for a binary hard-sphere mixture in the PY approximation have already been presented by Laird and Haymet for three values of the size ratio ($\alpha = 0.8, 0.5, 0.33$) at three different concentrations ($x_1 = 0.2, 0.5, 0.8$) [27]. However, the guiding philosophy of the above authors was that of verifying how good an estimate of the total excess entropy is obtained if one resorts only to the two-body term. In this paper we propose a different 'reading' that is based, instead, on a careful inspection of the behaviour of the residual multiparticle entropy Δs as a function of the number density and of the relative concentration of the two species. One further difference between the present calculations and those reported in [27] lies in the choice of the equation of state (EOS) that is used for the evaluation of the total excess entropy. In fact, Laird and Haymet used a version of the Mansoori–Carnahan–Starling–Leland EOS [28] modified by Kranendonck and Frenkel [26]. This phenomenological recipe for the EOS of the mixture does indeed provide a very accurate fit of the simulation data. However, our present goal is not so much that of pursuing a close quantitative correspondence with the numerical experiments. Instead, we intend to perform a critical comparison between the information on Δs, which can be autonomously gathered within the PY framework, and the current knowledge on the phase diagram of the mixture. Therefore, in order to avoid the risk of *unbalancing* the 'local' estimate of Δs through an input for s_{ex} that would be spurious to the PY recipe, we followed an *internal* route to the EOS of the mixture, specifically that provided by the density-fluctuation theorem. This choice, as opposed to the alternative one that stems from the virial theorem, can be formally justified on some rather general grounds, independently of its better quantitative agreement with the exact EOS. In fact, it can be shown that in a variational scheme it is the 'fluctuation' pressure that self-consistently descends from the stationarity property of the functional leading to the PY approximation [29]. Furthermore, at variance with the compressibility route, the 'virial' expression for the partial chemical potential of the ith species does *not* asymptotically reduce to the exact expression for the work of putting one single particle of species i into the multicomponent fluid in the limit where the radius of the inserted particle grows to infinity [30].

We also carried out some test calculations using the Lee and Levesque (LL) analytical representation of the radial distribution functions obtained through Monte Carlo simulations [31]. The results corroborated the overall reliability of the trends given by the PY approximation.

As far as the technical details of the calculations are concerned, after Fourier inverting the analytical expressions for the partial structure factors, we obtained the radial distribution functions $g_{ij}(r)$ over a range $\mathcal{R}_{max} \simeq 31\sigma$ with a spatial resolution $\Delta r \simeq 1.2 \times 10^{-4}$. With such values for $\mathcal{R}_{max}$ and Δr, we found that the numerical integrations needed for the calculation of s_2 were sufficiently stable at the third decimal place all over the explored

space of parameters. The total excess entropy s_{ex} follows analytically from equations (2.7), (2.8) and (2.13) of [30]. We estimated that the numerical error affecting Δs did not exceed 0.005 in the most delicate regime corresponding to highly asymmetric sizes and rather dilute concentrations of the larger-sized spheres.

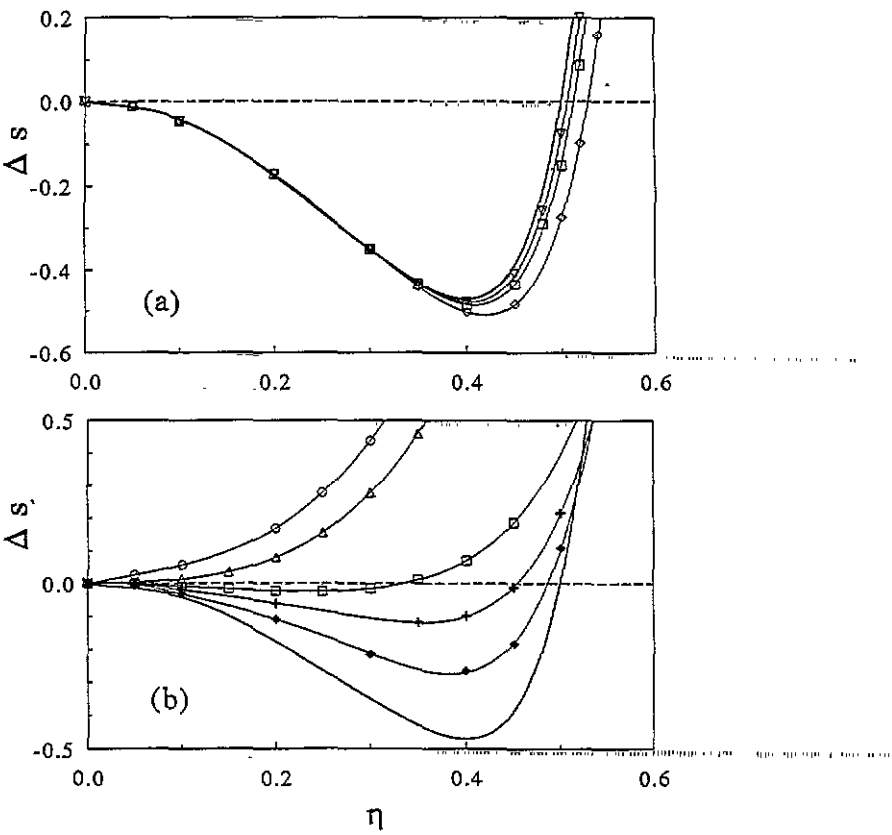

Figure 1. *Residual multiparticle entropy $\Delta s(\eta, x_1; \alpha)$ plotted as a function of the total packing fraction η for two values of the size ratio: (a) $\alpha = 0.85$; (b) $\alpha = 0.1$. The curves refer to different values of the larger-particle mole fraction and are labelled as follows: circles, $x_1 = 10^{-3}$; triangles, $x_1 = 10^{-2}$; squares, $x_1 = 10^{-1}$; crosses, $x_1 = 0.3$; open diamonds, $x_1 = 0.4$; full diamonds, $x_1 = 0.6$; downward triangles, $x_1 = 0.9$. The unlabelled full curve represents the corresponding PY result in a single-component hard-sphere fluid.*

The resulting difference $\Delta s(\eta, x_1; \alpha)$, when plotted as a function of the total packing fraction η for assigned values of α and x_1, has a shape similar to that found in a monodisperse hard-core fluid [17]. Figure 1 shows the residual multiparticle entropy for two values of the size ratio ($\alpha = 0.1, 0.85$) and for a number of increasing mole fractions of the larger spheres. As discussed in section 1, we trace the locus of points $\eta_0(x_1; \alpha)$ where Δs changes sign. We anticipate that the behaviour of η_0 as a function of x_1 is distinctively different according to whether the size ratio α is smaller or bigger than ≈ 0.22. In fact, as is seen from figure 1(*b*), in the strongly asymmetric regime the negative well of Δs becomes wider and deeper for increasing values of x_1, eventually shaping into the outermost single-component profile. Correspondingly, the quantity $\eta_0(x_1; \alpha)$ increases monotonically with x_1 up to the

'pure' hard-sphere threshold $\eta_0^{(HS)} \simeq 0.499$ (a value that is consistently calculated within the PY approximation). On the other hand, for $\alpha = 0.85$, the dependence of Δs upon x_1 is neatly resolved only for densities beyond the minimum ($\eta_{min} \simeq 0.4$). Furthermore, for mole fractions of the larger spheres strictly less than one, the residual-entropy curves lie systematically beneath the single-component result. Consequently, $\eta_0(x_1;\alpha)$ turns out to be larger than $\eta_0^{(HS)}$. One can also appreciate from figure 1 that the above quantity shows a 're-entrant' behaviour as x_1 grows from zero to one.

3. Results

The overall efficiency in the way a number of non-overlapping spheres with two different sizes distribute, on the average, onto the available space is the key factor that rules the statistical geometry of the model. As such, the sphere-size ratio plays a critical role in fixing the shape of the phase diagram.

In what follows, we organize the presentation of the results into three subsections, two of which are devoted to a discussion of the opposite regimes of grossly similar and very dissimilar radii. In the third subsection we focus on the properties of an equimolar mixture over the entire range of sphere-size ratios.

3.1. Close size-similarity regime: solid–fluid phase equilibria

Computer simulation studies of the phase diagram have recently been performed for diameter ratios in the range $0.85 \leqslant \alpha \leqslant 1$ [2]. In this regime, obvious 'continuity' reasons with the phase behaviour of the pure system formed by equal-sized spheres ($\alpha = 1$) clearly suggest that the dense mixture eventually freezes into a substitutionally disordered FCC or HCP crystal, in which particles of the two species are distributed irregularly over the sites of the underlying lattice. As the size ratio is varied from 1 to 0.85, the originally spindle character of the solid–liquid co-existence curve is found to change over to an azeotropic type and, eventually, into a eutectic diagram. Density-functional theories predict that the solubility of the larger spheres in the crystal of predominantly smaller spheres vanishes for $\alpha < 0.85$ [7, 11].

The thermodynamic stability of more complex solid structures (such as the hexagonal AB_2 phase or the cubic AB_{13} phase, whose central body consists of an icosahedral cluster formed by 13 small spheres) has also been investigated [1, 3].

Typical radial distribution functions of the mixture in this regime are shown in [26]. In figure 2 we compare the locus of points where Δs changes sign, i.e. $\eta_0(x_1;\alpha)$, with the total packing fraction of the mixture at the freezing point, $\eta_f(x_1;\alpha)$, for three sample size ratios in the range $0.85 \leqslant \alpha \leqslant 1$. The composition dependence of $\eta_0(x_1;\alpha)$ turns out to be broadly consistent with the behaviour of $\eta_f(x_1;\alpha)$. The ordering threshold of the mixture, as is resolved by the residual multiparticle entropy, falls almost systematically slightly beyond the freezing line. However, what catches the eye more than the rather small quantitative discrepancy, which for $\alpha = 0.85$ never exceeds 3.3%, is the absence in $\eta_0(x_1;\alpha)$ of any cusp singularity at low values of x_1. Such a feature is notoriously associated with the genesis of a eutectic point in the phase diagram of sufficiently asymmetric mixtures. On the other hand, upon decreasing the size ratio, the maximum in $\eta_0(x_1;\alpha)$ slides towards smaller mole fractions of the larger spheres as correspondingly does the maximum in $\eta_f(x_1;\alpha)$.

The results presented in figure 2 clearly demonstrate that the locus of points traced through the zero of the residual multiparticle entropy is very closely related to the thermodynamic phase boundary of the homogeneous fluid phase. The existence of an

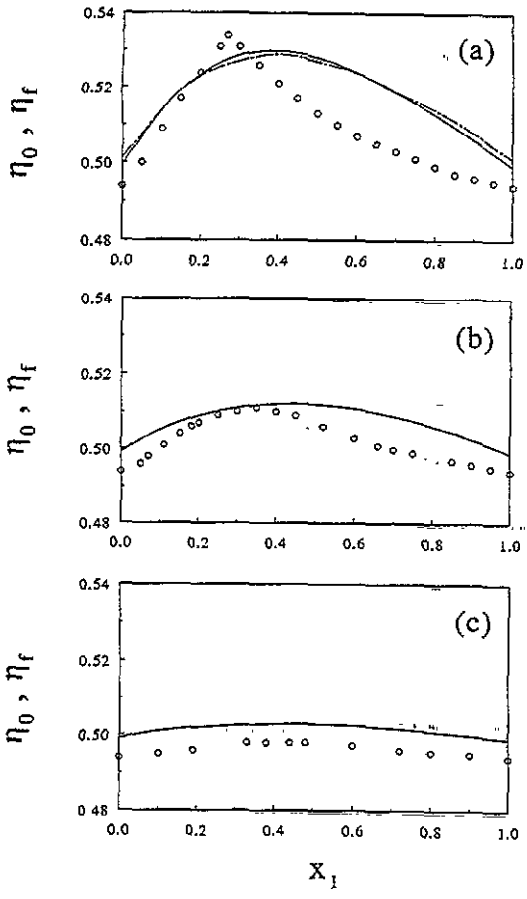

Figure 2. The locus of points $\eta_0(x_1;\alpha)$ where $\Delta s(\eta, x_1;\alpha) = 0$, plotted as a function of the larger-particle mole fraction x_1 for three values of the size ratio: (*a*) $\alpha = 0.85$; (*b*) $\alpha = 0.90$; (*c*) $\alpha = 0.95$. The theoretical result is shown as a full curve and is compared with the corresponding simulation data for the freezing point of the mixture (circles) which have been extracted from figure 8 of [2]. The prediction for $\eta_0(x_1;\alpha)$ obtained through the Lee and Levesque parametrization scheme [31] is also shown in (*a*) as a chain curve.

intrinsic threshold in the fluid phase, correlated with the freezing density, has also recently been postulated by Rosenfeld through an analysis, carried out for a large spectrum of potentials, of a 'critical' instability manifested by the hyper-netted-chain (HNC) approximation with respect to the diagrammatic iteration process [6]. His results for the binary hard-sphere mixture are qualitatively consistent with the shape of $\eta_0(x_1;\alpha)$.

The quantitative differences between $\eta_0(x_1;\alpha)$ and $\eta_f(x_1;\alpha)$ cannot be solely ascribed to the PY approximation, whose overall reliability is largely confirmed by comparison with the results obtained through the LL parametrization of the simulation data. One such comparison is reported in figure 2(*a*) for $\alpha = 0.85$. On the other hand, as already noted in section 1, such differences might well be intrinsic to the 'one-phase' character of the criterion we are exploiting. We should also remark that, within the present theoretical framework, the system is described as a homogeneous and isotropic mixture of two species. Therefore, any reliable inference on a transformation that leads to a phase separation of the fluid into two co-existing solids with different concentrations (as is the case for the eutectic point) is likely to be beyond the limits of the present scheme. This may explain why the criterion misses the expected evolution towards a eutectic behaviour.

3.2. The highly asymmetric regime

The landmark value of the sphere-size ratio for the strongly asymmetric regime is about 0.2. In fact, Biben and Hansen, using the Rogers–Young closure, predicted that for $\alpha \lesssim 0.2$

a binary mixture would separate into two fluid phases if the volume fractions occupied by the two particle species were roughly comparable [5]. This result was later confirmed by Lekkerkerker and Stroobants [32] and, most recently, by Rosenfeld [33] with different theoretical approaches. Indeed, a demixing transition has been observed in mixtures of colloidal particles of two different sizes [16]. Evidence of entropy-driven demixing has been also presented in a computer simulation study of an additive mixture of large and small cubes on a lattice [34].

As is well known, the PY approximation does not predict a macroscopic phase separation of a binary hard-sphere mixture into two disordered phases [30]. Nevertheless, the 'osmotic depletion' effect, which is responsible for the appearance of a miscibility gap, is already built into the PY closure [33]: in fact, in the limit of vanishing size ratios, a very sharp and narrow peak builds up near contact in the PDF of the larger spheres [4]. However, the increase of $g_{11}(\sigma_1)$ as $\alpha \to 0$ is not strong enough to induce divergent concentration fluctuations in the long-wavelength limit.

The density behaviour of the residual multiparticle entropy in the strongly asymmetric regime is much more sensitive to variations of the relative concentration of the two species than is found in the opposite regime of radii that are not very dissimilar. As is seen from figure 1(*b*), upon lowering the mole fraction of the larger spheres, the well depth reduces while the position of the minimum shifts to lower values of η. In particular, for $\alpha \lesssim 0.14$, the minimum eventually disappears (to within the numerical precision of the calculation) as x_1 drops below ~ 0.03: correspondingly, for lower values of the concentration, Δs is found to be everywhere *positive* and to increase *monotonically* with the total packing fraction of the mixture†. Following the discussion made in section 1 on the rationale of the ordering criterion based on the residual multiparticle entropy, it turns out to be natural to associate such a 'switch' in the behaviour of Δs against η with the genesis of a different type of order in the mixture. The presently estimated threshold in the relative concentration of the two species falls close to the region where the mixture is expected to demix into two fluid phases. In fact, we recall that Biben and Hansen predicted a 'critical' concentration of the larger spheres, below which phase separation occurs, of about 0.02 for $\alpha = 0.1$ [5], while Rosenfeld predicts a value about one order of magnitude lower [33].

In figure 3 we present our results for the loci where $\Delta s(\eta, x_1; \alpha) = 0$. The data show a sharp change of behaviour in the compositional dependence of $\eta_0(x_1; \alpha)$ for $\alpha \lesssim 0.2$. In fact, we find that in this range of size ratios the function $\eta_0(x_1; \alpha)$ lies below the 'pure' hard-sphere threshold all over the concentration range explored and increases monotonically with x_1. The loci where the residual entropy vanishes correspond to states of the mixture that are far enough away, as far as the relative concentration of the two species is concerned, from the structural condition described above in relation to the phenomenon of fluid–fluid demixing. In fact, in the range of parameters exploited in figure 3, the density profile attained by the larger spheres is almost unaffected by the presence of the smaller-particle component. Figure 4 shows the density evolution of the three PDF for $\alpha = 0.2$ and $x_1 = 0.1$. The feature that visibly emerges for $\eta \gtrsim 0.431$ (namely, where Δs becomes positive) is a second-neighbour maximum in $g_{22}(r)$, whose position is shifted with respect to the close-contact distance σ_2 by an amount equal to σ_1. We surmise that the vanishing of the residual multiparticle entropy signals the incipient short-range ordering of the smaller spheres, a process that appears to be 'ruled' by the larger-sphere component. We recall that the largest relative size of a particle that may fit inside the cavity formed by four touching spheres

† A more definite statement on the functional behaviour of Δs in this range of parameters will call for an analytical expansion of the theory in the limit of very small packing fractions.

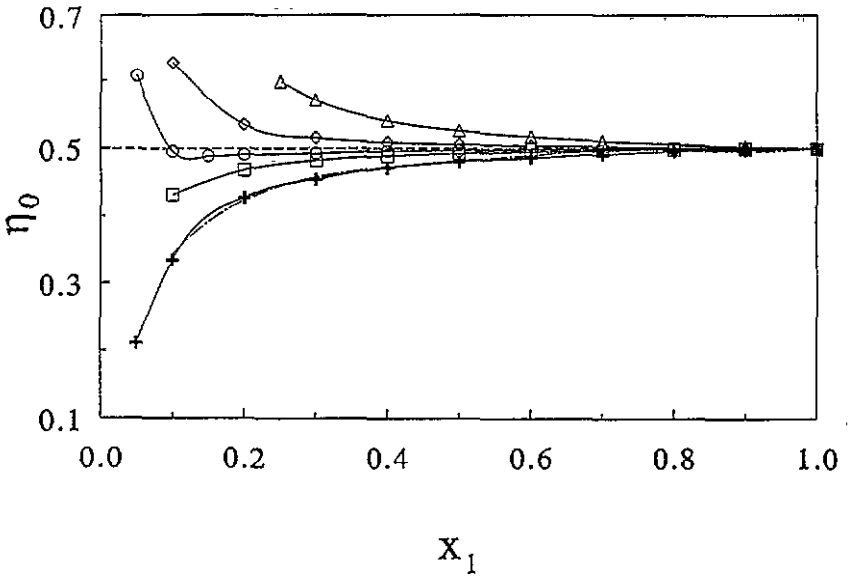

Figure 3. The locus of points $\eta_0(x_1;\alpha)$ where $\Delta s(\eta, x_1;\alpha) = 0$, plotted as a function of the larger-particle mole fraction x_1 in the highly asymmetric size-ratio regime: crosses, $\alpha = 0.1$; squares, $\alpha = 0.2$; circles, $\alpha = 0.22$; diamonds, $\alpha = 0.25$; triangles, $\alpha = 0.3$. The prediction for $\eta_0(x_1;\alpha)$ obtained through the Lee and Levesque parametrization scheme [31] is also shown for $\alpha = 0.1$ as a chain curve.

(in a basic tetrahedral arrangement) is $\frac{1}{2}\sqrt{6} - 1 \simeq 0.225$. One may thus expect that for α less than such a value, the average spatial distribution of the larger spheres will not be affected in a sensitive way—even at moderately high densities—by the presence of the smaller spheres. In fact, their size is such that they can be easily accommodated within the interstitial holes that are left over in the structural pattern that is autonomously built up by the larger particles. This conclusion can be readily checked through the comparison of $g_{11}(r)$ with the PDF of a one-component fluid of spheres with diameter σ_1 which occupy the same volume fraction as the larger spheres in the mixture. As is seen from figure 4(*c*), the only relevant difference that is resolved for $\alpha = 0.2$ between the two PDF is the expected increase of the value attained by $g_{11}(r)$ at contact. Apart from this, the profile of this function in the mixture closely reproduces the corresponding profile in the 'equivalent' pure fluid. However, upon increasing the relative size of the smaller spheres up to a value of just 0.3 while still keeping $\eta = 0.5$, the profile of the first coordination shell in $g_{11}(r)$ visibly distorts. As can be appreciated from figure 5, the function drops after contact much faster than in the pure fluid: a secondary minimum appears that is followed by a new satellite peak at a relative distance $(\sigma_1 + \sigma_2)$. Correspondingly, a maximum shows up in $g_{22}(r)$ at a distance $\sim 2\sigma_2$. These features clearly indicate that, for $\alpha \gtrsim 0.2$, the smaller-particle component distinctly interferes with the packing of the larger spheres: as a result, the local density profile becomes modulated by *two* spatial periodicities, which are fixed by the sizes of both species.

The relative ordering of the two species in the fluid phase is attained through a continuous structural change, which is clearly resolved in the *fine structure* of the configurational entropy but is not strong enough to affect the thermodynamics of the mixture. This process preludes the freezing of the mixture into a solid phase. In fact, upon increasing

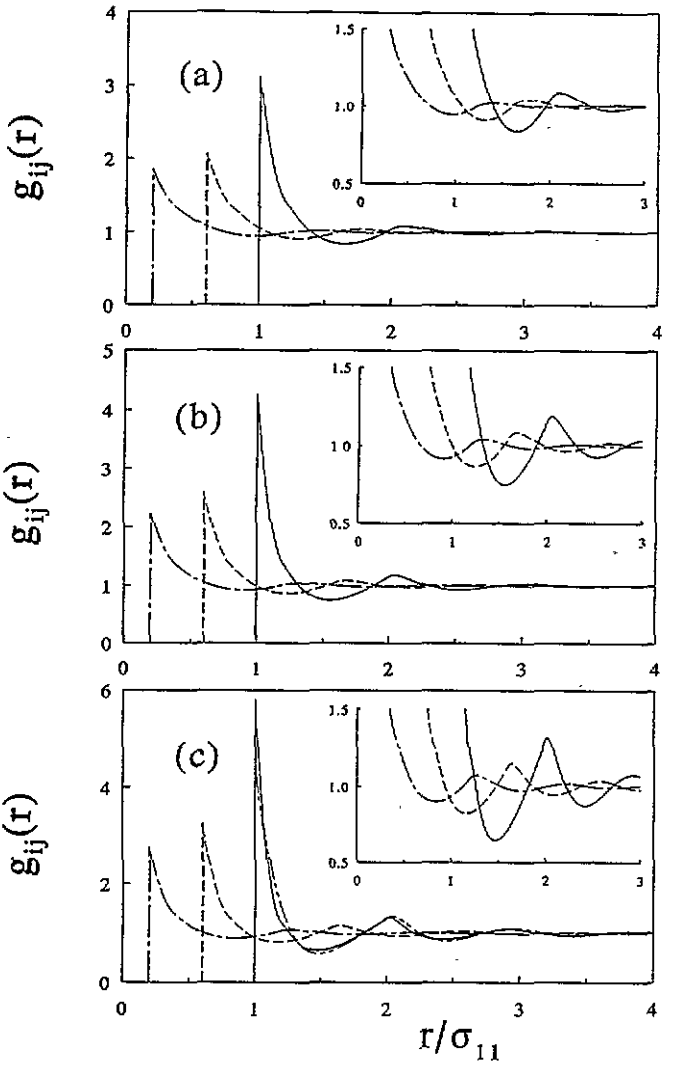

Figure 4. Radial distribution functions $g_{ij}(r)$, plotted as a function of r/σ_{11}, for $\alpha = 0.2$, $x_1 = 0.1$ and for three values of the total packing fraction: (*a*) $\eta = 0.35$; (*b*) $\eta = 0.43$; (*c*) $\eta = 0.5$. The double-dot chain curve in (*c*) represents the PDF of a one-component fluid of hard spheres with diameter σ_1 occupying the same volume fraction as the larger spheres in the mixture ($\eta_1 = 0.467$). The inset shows a magnification of the short-range structure.

the mole fraction of the larger particles, the freezing threshold of the mixture will settle onto the pure-liquid value and, correspondingly, the 'distance' between the two boundaries will progressively close up (see figure 3).

3.3. The case of an equimolar mixture

In this section we shall ultimately focus on the phase diagram of a mixture whose concentration ratio is kept fixed at a value 1 : 1. Figure 6 shows $\eta_0(x_1;\alpha)$ plotted as a function of α for $x_1 = \frac{1}{2}$. In the range of size ratios $0.50 \lesssim \alpha \lesssim 0.75$, the PDF of the larger-sized spheres becomes negative in the region of the first dip for a density that corresponds to a value of the residual multiparticle entropy that is still negative but very close to zero. Actually, the break-point of the approximation is found to lie beyond the minimum undergone by Δs, i.e. along the rapidly increasing branch of the curve (see figure 1). One may tentatively 'bridge' the gap in $\eta_0(x_1;\alpha)$ by extrapolating Δs up to its close intercept with the η axis: the results are shown in figure 6 as a broken curve.

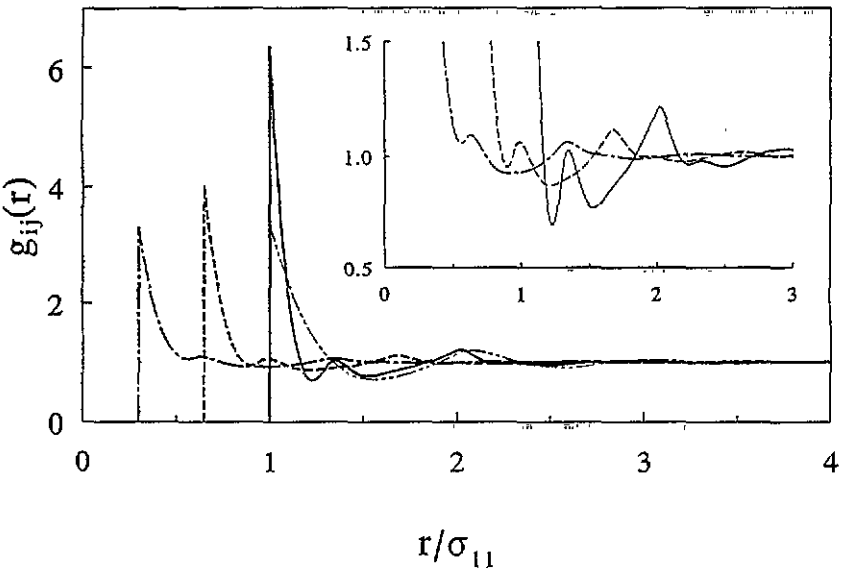

Figure 5. Radial distribution functions $g_{ij}(r)$, plotted as a function of r/σ_{11}, for $\alpha = 0.3$, $x_1 = 0.1$ and $\eta = 0.5$. The double-dot chain curve represents the PDF of a one-component fluid of hard spheres with diameter σ_1 occupying the same volume fraction as the larger spheres in the mixture ($\eta_1 = 0.403$). The inset shows a magnification of the short-range structure.

Upon decreasing the value of α from one, the ordering threshold monitored by Δs is initially raised towards higher values of the total packing fraction, consistent with the trend ascertained by the numerical simulation experiments. We also report in figure 6 the predictions given by two different density-functional theories. The chain curve is the outcome of a weighted-density-functional approach in the form set up by Denton and Ashcroft. This curve represents the total packing fraction of the fluid equimolar mixture at co-existence with a *disordered* FCC crystal for $1 > \alpha > 0.76$, and with a *pure* FCC solid (composed of larger spheres only) for lower size ratios†. It is worth emphasizing that in this latter case the global composition of the mixture after freezing is no longer equimolar: in fact, the higher-density state is that of a pure solid in equilibrium with a binary fluid that is now confined onto a smaller volume.

The open symbols refer instead to an equimolar mixture of oppositely charged hard spheres *at infinite temperature* [8]. In this limit, the Coulomb interactions are ineffective but for imposing a condition of overall charge neutrality. Thus, at variance with the previous case, the relative compositions of the two species are constrained to attain the same value even in the solid phases. The theory of Brami and co-workers predicts disjoint stability domains for three different solid structures, namely the compositionally disordered FCC crystal, the NaCl structure formed by two interpenetrating FCC lattices, and the CsCl structure, a variant of the body-centred cubic structure where a small sphere lies in the centre position of the unit cubic cell formed by eight larger particles. According to the above theory, the disordered FCC is stable in the range $1 > \alpha > 0.85$, the CsCl structure in the range $0.75 > \alpha > 0.70$, and the NaCl structure in the range $0.46 > \alpha > 0.33$.

† This curve was obtained from figure 9 of [11] via the density of the larger spheres in the fluid mixture at co-existence with the solid.

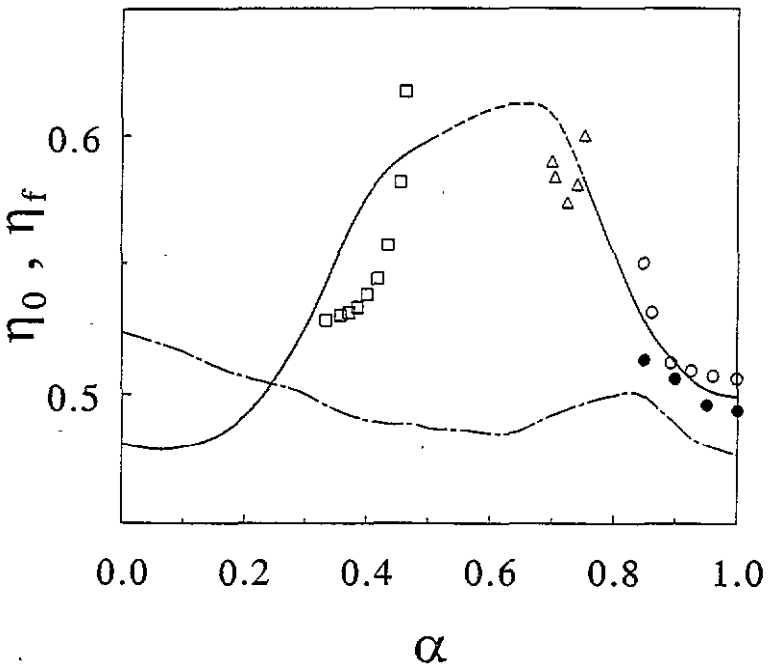

Figure 6. The locus of points $\eta_0(x_1;\alpha)$ where $\Delta s(\eta, x_1;\alpha) = 0$, plotted as a function of the size ratio α for an equimolar mixture. The theoretical result is shown as a full curve. The broken curve corresponds to an extrapolation of the intercept of Δs with the η axis in the range of parameters where the PDF of the larger-sized spheres goes negative before Δs becomes positive. We also show the available data for the freezing point of the mixture, calculated through computer simulation (full circles) [2] and via two different density functional theories. The chain curve was obtained from figure 9 of [11]. Open circles, triangles and squares represent the freezing thresholds of a charged fluid equimolar mixture at infinite temperature co-existing with a compositionally disordered FCC lattice, with a NaCl-type structure, and with a CsCl-type structure, respectively [8].

For values of α intermediate between the three stability ranges, no zero is found in the difference between the grand potential of the fluid and that of any trial solid phase (among those cited above).

On the other hand, the CsCl and NaCl structures turn out to be metastable in the theory of Denton and Ashcroft. Indeed, the greater stability over a very wide range of concentrations of a pure solid, precipitated by the larger spheres, in equilibrium with a two-component fluid is confirmed by the recent simulation of a mixture with size ratio $\alpha = 0.58$ [1].

As far as the present analysis is concerned, it is clear from figure 6 that the shape of $\eta_0(x_1;\alpha)$ is broadly consistent with the 'topology' of the freezing points found by Brami and co-workers. Even the gap that opens up in $\eta_0(x_1;\alpha)$ as a consequence of the physical breakdown of the PY approximation might be related, even if somewhat indirectly, to the stability gap registered between the CsCl and NaCl structures. The correspondence between the present theory and the results found by Brami and co-workers is, *a posteriori*, not all that surprising: in fact, by construction, the present entropic criterion actually resolves the onset of those ordering phenomena that drive the system to a state with the same composition as the parent disordered phase.

On the basis of the above argument, it would be natural to argue that the freezing line

obtained by Denton and Ashcroft should systematically lie below the locus $\eta_0(x_1;\alpha)$. As is seen from figure 6, this turns out to be the case for $\alpha \gtrsim 0.22$ only, where the two curves intersect. Hence, granted that the weighted-density-functional theory correctly predicts the nature of the fluid–solid co-existence even in this highly asymmetric regime, we surmise that the crossover undergone by the two curves is to be related with the possibility that some other efficient spatial organization of the two species may stabilize the fluid phase over a wider density range than in the pure system. In fact, as already emphasized in the preceding section, it is precisely for $\alpha \lesssim 0.22$ that the dense fluid mixture achieves an 'optimal' structural condition where the smaller spheres can actually fit inside the interstices formed by the larger particles. This state, while still being homogeneous, possesses a high degree of short-range order as to the relative spatial distribution of the two species. As such, it is likely to be competitive with a non-homogeneous state of the mixture where a pure solid co-exists with a binary fluid. We argue that this fact may indeed account for the more extended stability range, along the η axis, of the fluid phase in the strongly asymmetric size-ratio regime: the solid phase happens to be 'delayed' until when even the inter-species ordering of the fluid phase no longer pays enough in terms of global packing efficiency.

4. Concluding remarks

The partial resolution of the configurational entropy into contributions arising from n-body spatial correlations leads to an intermediate statistical-thermodynamical picture that is based on the behaviour of the residual multiparticle entropy Δs as a function of the parameters that characterize the equilibrium state of the fluid. This quantity is obtained from the total entropy of the fluid after subtraction of a (qualitatively uninteresting) *background* value that is constructed as the sum of the ideal and pair terms. As such, Δs conveys a type of information that is intermediate between the purely macroscopic level and the fully statistical-mechanical description of the system, and may be used as a sort of 'litmus paper' so as to unveil those more or less hidden features of the phase behaviour that are specifically ascribable to triplet or higher-order correlations.

The primary motivation for this study was that of exploiting the usefulness of such an indicator in the case of a more complex model than previously investigated, namely a binary mixture composed of different relative concentrations of unequal hard spheres. In this regard, we have found rather unambiguous interrelations between the most appariscent phenomena that occur in the mixture (freezing, phase separation) and the thermodynamic behaviour of $\Delta s(\eta, x_1; \alpha)$ in the fluid phase.

On the basis of the present results, it seems fair to conclude that the residual multiparticle entropy contains a germinal indication of the phase transformations that take place in the system. The generality of this statement has also recently been checked in the case of the gas–liquid phase transition [35]. The analysis of Δs for both a Lennard-Jones and a hard-core Yukawa fluid shows that this quantity sharply blows up to positive values on both sides of the spinodal region. More interestingly, the criterion accounts for both the gas–liquid and freezing transitions and even predicts the existence of a point in the thermodynamic space of the metastable liquid phase that actually unveils as an intrinsic underlying signature of the triple-point phase coexistence.

We plan to extend the present study to a binary mixture with more realistic interatomic potentials in a forthcoming paper.

Acknowledgments

This work was supported by the Ministero dell'Università e della Ricerca Scientifica e Tecnologica (MURST) and by the Consorzio Interuniversitario Nazionale di Fisica della Materia (INFM), Italy.

References

[1] Eldridge M D, Madden P A and Frenkel D 1993 *Nature* **365** 35
[2] Kranendonck W G T and Frenkel D 1991 *Mol. Phys.* **72** 679
[3] Eldridge M D, Madden P A and Frenkel D 1993 *Mol. Phys.* **79** 105; *Mol. Phys.* **80** 987
[4] Biben T and Hansen J-P 1990 *Europhys. Lett.* **12** 347
[5] Biben T and Hansen J-P 1991 *Phys. Rev. Lett.* **66** 2215; 1991 *J. Phys.: Condens. Matter* **3** 65
[6] Rosenfeld Y 1992 *Phys. Rev.* A **46** 4922
[7] Barrat J L, Baus M and Hansen J-P 1986 *Phys. Rev. Lett.* **56** 1063; 1987 *J. Phys. C: Solid State Phys.* **20** 1413
[8] Brami B, Joly F, Barrat J L and Hansen J-P 1988 *Phys. Lett.* **132A** 187
[9] Rick S W and Haymet A D J 1989 *J. Chem. Phys.* **90** 1188
[10] Zeng X C and Oxtoby D W 1990 *J. Chem. Phys.* **93** 4357
[11] Denton A R and Ashcroft N W 1990 *Phys. Rev.* **42A** 7312
[12] Xu H and Baus M 1992 *J. Phys.: Condens. Matter* **4** L663
[13] Pusey P N 1991 *Liquids, Freezing and Glass Transition* ed J-P Hansen, D Levesque and J Zinn-Justin (Amsterdam: North-Holland) p 763
[14] Bartlett P, Ottewill R H and Pusey P N 1990 *J. Chem. Phys.* **93** 1299
[15] Bartlett P, Ottewill R H and Pusey P N 1992 *Phys. Rev. Lett.* **68** 3801
[16] Sanyal S, Easwar N, Ramaswamy S and Sood A K 1992 *Europhys. Lett.* **18** 107
van Duijneveldt J S, Heinen A W and Lekkerkerker H N W 1993 *Europhys. Lett.* **21** 369
Kaplan P D, Rouke J L, Yodh A G and Pine D J 1994 *Phys. Rev. Lett.* **72** 582
[17] Giaquinta P V and Giunta G 1992 *Physica* A **187** 145
[18] Giaquinta P V, Giunta G and Prestipino Giarritta S 1992 *Phys. Rev.* A **45** 6966
[19] Caccamo C, Giaquinta P V and Giunta G 1993 *J. Phys.: Condens. Matter* **5** 75
An application of the entropy criterion to the prediction of the phase diagram of C_{60} has been recently made: Cheng A, Klein M L and Caccamo C 1993 *Phys. Rev. Lett.* **71** 1200
[20] Hernando J A 1990 *Mol. Phys.* **69** 319
[21] Uhlenbeck G E 1968 *Fundamental Problems in Statistical Mechanics II* ed E G D Cohen (New York: Wiley)
Fisher M E 1972 *Essays in Physics* vol 4 ed G K T Conn and G. N Fowler (New York: Academic)
[22] Ackerson B J 1993 *Nature* **365** 11
[23] Percus J K and Yevick G J 1959 *Phys. Rev.* **110** 1
[24] Lebowitz J L 1964 *Phys. Rev.* A **133** 895
[25] Fries P H and Hansen J-P 1983 *Mol. Phys.* **48** 891
[26] Kranendonck W G T and Frenkel D 1991 *Mol. Phys.* **72** 715
[27] Laird B B and Haymet A D J 1992 *J. Chem. Phys.* **97** 2153
[28] Mansoori G A, Carnahan N F, Starling K E and Leland T W Jr 1971 *J. Chem. Phys.* **54** 1523
[29] Baxter R J 1967 *J. Chem. Phys.* **47** 4855; 1971 *Physical Chemistry: An Advanced Treatise* ed H Eyring, D Henderson and W Jost (New York: Academic) p 332
[30] Lebowitz J L and Rowlinson J S 1964 *J. Chem. Phys.* **41** 133
[31] Lee L L and Levesque D 1973 *Mol. Phys.* **26** 1351
[32] Lekkerkerker H N W and Stroobants A 1993 *Physica* A **195** 387
[33] Rosenfeld Y 1994 *Phys. Rev. Lett.* **72** 3831
[34] Dijkstra M and Frenkel D 1994 *Phys. Rev. Lett.* **72** 298
[35] Giaquinta P V, Giunta G and Malescio G 1994 *Entropy versus correlations in simple fluids: the gas-liquid phase transition* to be published